Generalized distorted-wave Born approximation for neutron reflection

V. F. Sears
Atomic Energy of Canada Limited Research, Chalk River, Ontario, Canada K0J 1J0
(Received 13 August 1993)

A theory is developed for the specular reflection of thermal neutrons from an arbitrary smooth surface or interface using a Green-function technique and leads to a family of Born approximations that includes both the familiar plane-wave Born approximation (PWBA) and a generalized distorted-wave Born approximation (DWBA). The DWBA reduces to the PWBA if the wave-vector transfer, q_z, is much larger than the critical wave vector for total reflection, q_c, and to Fresnel's formula for reflection from a sharp surface if q_z is much less than the inverse surface thickness. Detailed numerical calculations of the reflectivity for a number of symmetric model surfaces show that it is only when $q_z \gg q_c$ that the reflectivity R is sensitive to the detailed shape and thickness of the surface potential. In particular, one requires experiments with q_z/q_c ranging from about 3 to 30, where R decreases from about 10^{-3} to 10^{-7}, to obtain useful information on the shape and thickness of symmetric surfaces. From a comparison with the exact reflectivity for one particular surface, we find that the DWBA is typically three orders of magnitude more accurate than both the PWBA and an *ad hoc* model commonly used by experimenters for all values of q_z, and that the relative error in the DWBA is almost everywhere less than 0.01% which is, therefore, of the same order of magnitude as the intrinsic error in the Fermi pseudopotential itself. The high accuracy that we have found when the DWBA is applied to symmetric surfaces is in contrast to the relatively low accuracy that others have found when they applied this kind of approximation to thin films on substrates of low intrinsic reflectivity. The reason for this is discussed.

I. INTRODUCTION

In the past ten years neutron reflectometry has proven to be an increasingly useful technique for investigating the structural properties of surfaces and interfaces at the molecular level.[1–4] Most of the major neutron-scattering centers now have dedicated reflectometers that are being used for a wide variety of applications in physics, chemistry, biology, and materials science. The observed reflectivity depends on the way in which the bound coherent scattering length density $f(z)$ varies with depth z in the neighborhood of the surface. To interpret the reflectivity measurements a common approach is to model the surface using an approximate staircase representation for $f(z)$ which allows one to calculate the corresponding reflectivity numerically using, for example, the conventional matrix method.[5,6] Any free parameters in $f(z)$ can then be determined by fitting to the measured reflectivity curve.

Better insight into the factors that govern the reflectivity profile is obtained if one can calculate it analytically in terms of the assumed model for $f(z)$. At angles of incidence well above the critical angle for total reflection, where the reflectivity is sufficiently small that multiple scattering is negligible, one can use the conventional plane-wave Born approximation (PWBA) in which the interaction potential is treated as a perturbation. An alternative approach is to use a distorted-wave Born approximation (DWBA) in which the reflection from a sharp surface is taken as the zeroth approximation and dealt with exactly, while the difference between the exact potential and that for the sharp surface is taken as the perturbation. The DWBA usually provides a better description of the reflectivity, especially at small angles of incidence.

Various approaches to the DWBA have previously been developed for calculating the reflectivity of rough surfaces,[7–11] ferromagnetic surfaces,[12,13] and thin films on substrates.[14–16] In this paper we present a new formulation of the DWBA to describe the specular reflection of thermal neutrons from smooth but otherwise arbitrary surfaces or interfaces. We begin in Secs. II and III by developing a Green-function method that yields a formally exact expression for the reflected amplitude. This leads in Sec. IV to a family of Born approximations that includes both the PWBA and a generalized DWBA. For the particular case of a thin film on a substrate, this DWBA reduces to an expression obtained by earlier authors.[16] In Sec. V we also demonstrate that our DWBA reduces to the PWBA when the angle of incidence is well above the critical angle for total reflection, and that it reduces to Fresnel's formula when the effective surface thickness goes to zero. Detailed numerical calculations of the reflectivity are performed for a number of symmetric model surfaces in Sec. VI to exhibit the dependence of the reflectivity on the shape and thickness of $f(z)$. In addition, Airy's formula[5] (which provides an exact expression for the reflectivity of, for example, an ideal thin film on a substrate) is used as a benchmark to test the accuracy and range of validity of the PWBA, the DWBA, and a simple *ad hoc* model that was introduced some years ago by Pershan and Als-Nielsen,[17] and is often used to interpret x-ray and neutron reflectivity data.

II. REFLECTION OF NEUTRONS FROM A SURFACE

The coherent wave $\psi(\mathbf{r})$, which describes the coherent elastic scattering of thermal neutrons in macroscopic media and, hence, all neutron optical phenomena, satisfies a one-body wave equation[18]

$$\left\{-\frac{\hbar^2}{2m}\Delta+V(\mathbf{r})\right\}\psi(\mathbf{r})=E\psi(\mathbf{r}) , \tag{2.1}$$

in which m is the neutron mass, $E\equiv(\hbar k)^2/2m$ the incident-neutron energy, and $V(\mathbf{r})$ the optical potential that represents the effective interaction of the neutron with the system. To a good approximation,[18] the optical potential is given by the equilibrium value of the Fermi pseudopotential,

$$V(\mathbf{r})=\frac{2\pi\hbar^2}{m}f(\mathbf{r}) , \tag{2.2}$$

where $f(\mathbf{r})=\rho(\mathbf{r})b(\mathbf{r})$ is the bound coherent scattering length density, $\rho(\mathbf{r})$ being the average number of atoms per unit volume, and $b(\mathbf{r})$ the average bound coherent scattering length per atom. For a chemically homogeneous system, such as a liquid-vapor interface, $b(\mathbf{r})$ is constant, and the $\mathbf{r}$ dependence of $f(\mathbf{r})$ is due entirely to the variation of $\rho(\mathbf{r})$ in the neighborhood of the surface. However, for a heterogeneous system, such as a thin film (or a thin-film multilayer) on a substrate, $\rho(\mathbf{r})$ and $b(\mathbf{r})$ both depend on $\mathbf{r}$.

We are concerned specifically with the specular reflection of neutrons from a plane surface. The z direction is taken normal to the surface, and the surface is assumed to be smooth in the sense that $f(\mathbf{r})=f(z)$, independent of x and y. More generally, the effect of statistical surface roughness on the specular component of the reflected wave could be included implicitly in an effective $f(z)$, but the calculation of the additional diffuse reflection from rough surfaces would require that the three-dimensional nature of $f(\mathbf{r})$ be taken properly into account. In the present paper we confine our attention to specular reflection, and assume only that

$$f(z)\rightarrow\begin{cases}\rho b, & z\rightarrow\infty\\ 0, & z\rightarrow-\infty,\end{cases} \tag{2.3}$$

where ρ and b are the values in the bulk material or substrate. The shape of $f(z)$ is otherwise arbitrary. The solution of the wave equation (2.1) is then of the form

$$\psi(\mathbf{r})=\exp[i(k_x x+k_y y)]\chi(z) , \tag{2.4}$$

where

$$\left\{\frac{d^2}{dz^2}+k_z^2\right\}\chi(z)=4\pi f(z)\chi(z) , \tag{2.5}$$

and $\mathbf{k}=(k_x,k_y,k_z)$ is the incident-neutron wave vector.

It follows from property (2.3) that, as $z\rightarrow-\infty$, Eq. (2.5) reduces to a free-particle wave equation and, hence, that

$$\chi(z)\rightarrow\exp(ik_z z)+r\exp(-ik_z z) \tag{2.6}$$

in this limit, and

$$\psi(\mathbf{r})\rightarrow\exp(i\mathbf{k}\cdot\mathbf{r})+r\exp(i\mathbf{k}'\cdot\mathbf{r}) , \tag{2.7}$$

in which $\mathbf{k}'=(k_x,k_y,-k_z)$. The first term in the asymptotic wave function (2.7) represents the incident wave (normalized to unit amplitude), and the second term the reflected wave with relative amplitude r and wave vector $\mathbf{k}'$. The reflectivity, which is defined as the fraction of incident neutrons that are reflected, is then given by $R=|r|^2$. Since neutron momentum is conserved in the x and y directions, the momentum transfer is in the z direction: $\mathbf{q}\equiv\mathbf{k}-\mathbf{k}'=(0,0,q_z)$, where $q_z=2k_z$.

III. INTEGRAL FORM OF THE WAVE EQUATION

We begin by putting

$$f(z)=f_0(z)+f_1(z) , \tag{3.1}$$

where $f_0(z)$ is some as yet arbitrary unperturbed part of the scattering length density, and $f_1(z)$ is the perturbation. Then the wave equation (2.5) becomes

$$\mathcal{L}\chi(z)=4\pi f_1(z)\chi(z) , \tag{3.2}$$

where $\mathcal{L}$ is the following linear differential operator:

$$\mathcal{L}=\frac{d^2}{dz^2}+k_z^2-4\pi f_0(z) . \tag{3.3}$$

Let $\chi_0(z)$ denote the solution of the unperturbed wave equation,

$$\mathcal{L}\chi_0(z)=0 , \tag{3.4}$$

and $G(z,z')$ the solution of the equation

$$\mathcal{L}G(z,z')=4\pi\delta(z-z') \tag{3.5}$$

that represents an outgoing wave from the point $z=z'$, i.e., the retarded Green function. Then one can easily verify that the integral equation

$$\chi(z)=\chi_0(z)+\int_{-\infty}^{\infty}G(z,z')f_1(z')\chi(z')dz' \tag{3.6}$$

is equivalent to the original differential equation (3.2) and is a special case of the Lippmann-Schwinger equation in scattering theory.[18,19]

In general,

$$\chi_0(z)\rightarrow\exp(ik_z z)+r_0\exp(-ik_z z)\quad\text{as } z\rightarrow-\infty , \tag{3.7}$$

where r_0 is the unperturbed reflected amplitude, and

$$G(z,z')\rightarrow\frac{2\pi}{ik_z}\exp(-ik_z z)\chi_0(z')\quad\text{as } z\rightarrow-\infty . \tag{3.8}$$

Hence it follows that the solution of Eq. (3.6) has the asymptotic form (2.6) with

$$r=r_0+\frac{2\pi}{ik_z}\int_{-\infty}^{\infty}\chi_0(z)f_1(z)\chi(z)dz . \tag{3.9}$$

This is a formally exact expression for the reflected amplitude.[20]

IV. THE BORN FAMILY OF APPROXIMATIONS

The iterated solution of the integral equation (3.6) gives the Born series,[18]

$$\chi(z)=\chi_0(z)+\int_{-\infty}^{\infty} G(z,z')f_1'(z')\chi_0 z'dz'+\cdots , \quad (4.1)$$

and in the Born approximation we put $\chi(z)=\chi_0(z)$, in which case expression (3.9) for the reflected amplitude becomes

$$r=r_0+\frac{2\pi}{ik_z}\int_{-\infty}^{\infty}\chi_0(z)^2 f_1(z)dz . \quad (4.2)$$

There is clearly a whole family of "Born approximations," depending on how $f_0(z)$ is chosen. The basic idea is to choose it such that the effect of the perturbation $f_1(z)$ on $\chi(z)$ is small, subject to the requirement that the equations for $\chi_0(z)$ and $G(z,z')$ are exactly solvable.

A. Plane-wave Born approximation

Let us first put

$$f_0(z)=0, \quad f_1(z)=f(z) , \quad (4.3)$$

so that the entire scattering length density is regarded as the perturbation. Then (3.4) becomes a free-particle wave equation. Its solution is a plane wave,

$$\chi_0(z)=\exp(ik_z z) , \quad (4.4)$$

and the corresponding Green function is an outgoing wave from the point $z=z'$:

$$G(z,z')=\frac{2\pi}{ik_z}\exp(ik_z|z-z'|) . \quad (4.5)$$

Note that this expression has the asymptotic property (3.8). According to (4.4), $r_0=0$, and the expression (3.9) for the reflected amplitude now becomes

$$r=\frac{2\pi}{ik_z}\int_{-\infty}^{\infty}\exp(ik_z z)f(z)\chi(z)dz . \quad (4.6)$$

This is, of course, still an exact result. In the Born approximation, where $\chi(z)=\chi_0(z)$, it reduces to the familiar result[2,14,16,21]

$$r=\frac{4\pi}{iq_z}\int_{-\infty}^{\infty}\exp(iq_z z)f(z)dz , \quad (4.7)$$

in which $q_z=2k_z$ is again the z component of the momentum transfer. Thus in this "plane-wave" Born approximation (PWBA), the reflected amplitude is just the Fourier transform of the scattering length density. (It will be noted that, elsewhere in thermal neutron-scattering theory,[18,22] the term "Born approximation" always means the PWBA.)

B. Distorted-wave Born approximation

Let us now put

$$f_0(z)=\begin{cases}\rho b, & z>0\\ 0, & z<0,\end{cases} \quad (4.8)$$

so that the unperturbed scattering length density corresponds to a geometrically sharp surface. Then

$$\mathcal{L}=\begin{cases}\dfrac{d^2}{dz^2}+K_z^2, & z>0\\ \dfrac{d^2}{dz^2}+k_z^2, & z<0,\end{cases} \quad (4.9)$$

where

$$K_z^2=k_z^2-4\pi\rho b . \quad (4.10)$$

Alternatively, $K_z=n_z k_z$, where

$$n_z=\sqrt{1-(q_c/q_z)^2} , \quad (4.11)$$

in which $q_c^2=16\pi\rho b$, and $q_z=2k_z$ as before.

We look for a solution of the unperturbed wave equation (3.4) for which the incident wave is partially reflected and refracted at the origin:

$$\chi_0(z)=\begin{cases}t_0\exp(iK_z z), & z>0\\ \exp(ik_z z)+r_0\exp(-ik_z z), & z<0.\end{cases} \quad (4.12)$$

Since $\chi_0(z)$ and its first derivative must both be continuous at $z=0$, we then get the familiar Fresnel formulas[5]

$$r_0=\frac{1-n_z}{1+n_z}, \quad t_0=\frac{2}{1+n_z} . \quad (4.13)$$

The Green function is an outgoing wave from the point $z=z'$ that is also partially reflected and refracted at $z=0$. Since $G(z,z')$ and its first derivative must both be continuous at $z=0$, we then find, in agreement with earlier authors,[9,15] that

$$G(z,z')=\frac{2\pi}{ik_z}\begin{cases}\dfrac{1}{n_z}\exp[iK_z(z-z')]-\dfrac{r_0}{n_z}\exp[iK_z(z+z')], & 0<z'<z\\ \dfrac{1}{n_z}\exp[-iK_z(z-z')]-\dfrac{r_0}{n_z}\exp[iK_z(z+z')], & 0<z<z'\\ t_0\exp[-i(k_z z-K_z z')], & z<0<z'\\ \exp[-ik_z(z-z')]+r_0\exp[-ik_z(z+z')], & z<z'<0\\ \exp[ik_z(z-z')]+r_0\exp[-ik_z(z+z')], & z'<z<0\\ t_0\exp[i(K_z z-k_z z')], & z'<0<z .\end{cases} \quad (4.14)$$

Note in particular that

$$G(z,z')=\frac{2\pi}{ik_z}\exp(-ik_z z)\chi_0(z') \quad \text{if } z<z' \text{ and } z<0 , \tag{4.15}$$

so that, once more, the Green function has the general asymptotic property (3.8). Hence, in the present "distorted-wave" Born approximation (DWBA), expression (4.2) for the reflected amplitude becomes

$$r=r_0+\frac{2\pi}{ik_z}\int_0^\infty\{[\exp(-ik_z z)+r_0\exp(ik_z z)]^2 f_1(-z) +[t_0\exp(iK_z z)]^2 f_1(z)\}dz . \tag{4.16}$$

C. Thin film on a substrate

For the particular case of a thin film (or a thin-film multilayer) on a substrate it is natural to take $f_0(z)$ to be the scattering length density for the substrate, and $f_1(z)$ the scattering length density for the thin film. If the total thickness of the film is d, we then have $f_1(z)=0$ unless $-d<z<0$. The DWBA result (4.16) for the reflected amplitude then reduces to[16]

$$r=r_0+\frac{2\pi}{ik_z}\int_{-d}^0[\exp(ik_z z)+r_0\exp(-ik_z z)]^2 f_1(z)dz . \tag{4.17}$$

When people speak of the DWBA for reflection from smooth surfaces they usually mean an expression such as (4.17). To avoid confusion, we shall call (4.16) the generalized DWBA.

D. Fresnel reflectivity

Finally, we note for future reference that the unperturbed reflectivity is given by

$$R_0=|r_0|^2=\left|\frac{1-n_z}{1+n_z}\right|^2 . \tag{4.18}$$

In most materials the absorption is small enough that b can be taken to be real. It is also usually positive, in which case q_c is real and

$$R_0=1 \quad \text{if } q_z<q_c . \tag{4.19}$$

Thus q_c is the critical wave-vector transfer for total reflection. On the other hand, regardless of the sign of b,

$$R_0=\frac{1}{16}\left[\frac{q_c}{q_z}\right]^4+\frac{1}{16}\left[\frac{q_c}{q_z}\right]^6+\frac{7}{128}\left[\frac{q_c}{q_z}\right]^8+\cdots \quad \text{if } q_z>|q_c| . \tag{4.20}$$

V. SYMMETRIC SURFACE

A. Reflected amplitudes for a symmetric surface

In this section we investigate and compare some of the properties of the PWBA (4.7) and the generalized DWBA (4.16). We begin by putting

$$f(z)=\rho b\phi(z) , \tag{5.1}$$

in which $\phi(z)$ is the normalized scattering length density, which can be expressed as

$$\phi(z)=\int_{-\infty}^z s(z')dz' , \tag{5.2}$$

where

$$s(z)\equiv\frac{d\phi(z)}{dz}=\frac{1}{\rho b}\frac{df(z)}{dz} . \tag{5.3}$$

It then follows from (2.3) that

$$\phi(\infty)=\int_{-\infty}^\infty s(z')dz'=1, \quad \phi(-\infty)=0 . \tag{5.4}$$

In what follows we shall assume for simplicity that the surface is symmetric in the sense that $s(z)$ is a real, even function of z. We also introduce the auxiliary quantity

$$J(q_z)=2\int_0^\infty\exp(iq_z z)s(z)dz =\frac{2}{\rho b}\int_0^\infty\exp(iq_z z)\frac{df(z)}{dz}dz . \tag{5.5}$$

Let

$$J(q_z)=J'(q_z)+iJ''(q_z) , \tag{5.6}$$

where

$$J'(q_z)=2\int_0^\infty\cos(q_z z)s(z)dz =\int_{-\infty}^\infty\exp(iq_z z)s(z)dz \tag{5.7}$$

and

$$J''(q_z)=2\int_0^\infty\sin(q_z z)s(z)dz . \tag{5.8}$$

Finally, let

$$a^2=2\int_0^\infty z^2 s(z)dz=\int_{-\infty}^\infty z^2 s(z)dz \tag{5.9}$$

and

$$\xi_n a^n=2\int_0^\infty z^n s(z)dz, \quad n=0,1,2,\ldots, \tag{5.10}$$

so that $\xi_0=\xi_2=1$. The quantity a provides a measure of the "thickness" of the surface (or surface layer), while the quantities ξ_n characterize the detailed shape of the surface.

The PWBA expression (4.7) for the reflected amplitude now becomes

$$r=\frac{4\pi\rho b}{q_z^2}J'(q_z) , \tag{5.11}$$

and the DWBA expression (4.16) becomes

$$r=r_0+\frac{2\pi\rho b}{q_z^2}\left\{[J(-q_z)-1]-2ir_0[\xi_1 q_z a] -r_0^2[J(q_z)-1]+\frac{t_0^2}{n_z}[J(n_z q_z)-1]\right\} . \tag{5.12}$$

Note that the same function $J(q_z)$ determines the reflected amplitude in both the PWBA and DWBA.

B. Dimensionless variables

We demonstrate below that the reflected amplitude can be regarded as a function of two dimensionless variables:

$$x=(q_c/q_z)^2, \quad y=q_z a \ . \tag{5.13}$$

With these definitions, the PWBA (5.11) becomes

$$r=\frac{x}{4}J'(q_z) \ , \tag{5.14}$$

and the DWBA (5.12) becomes

$$r=r_0+\frac{x}{8}\left\{[J(-q_z)-1]-2ir_0[\xi_1 y] -r_0^2[J(q_z)-1]+\frac{t_0^2}{n_z}[J(n_z q_z)-1]\right\} . \tag{5.15}$$

Since $n_z=\sqrt{1-x}$, we see from (4.13) that r_0 and t_0 depend only on x, and from (5.5) that $J(q_z)$ depends only on y. Thus in both the PWBA and DWBA, $r=r(x,y)$.

C. Validity of the PWBA

We shall see in Sec. VI that the DWBA is sufficiently accurate for all q_z to be used as a basis for answering questions such as those posed in this section and Sec. V D. The variable x depends on the value of q_z relative to the critical wave vector q_c. If $x \ll 1$ the expression (5.15) for the DWBA has the expansion

$$r=\frac{x}{4}J'(q_z)+\frac{x^2}{8}\left[J(q_z)-\frac{q_z}{2}\frac{dJ(q_z)}{dq_z}-\frac{i}{2}\xi_1 y\right]+O(x^3) \ , \tag{5.16}$$

in which the first term is the PWBA (5.14), i.e., the contribution from single scattering, and the remaining terms give the contribution from multiple scattering. We see that as $x \to 0$ multiple scattering is negligible and the DWBA reduces to the PWBA. Thus the PWBA will be valid for essentially any surface as long as $q_z \gg q_c$.

D. Validity of Fresnel's formula

The variable y depends on the value of q_z relative to the surface thickness a. If $y \ll 1$ the expression (5.15) for the DWBA has the expansion

$$r=r_0-\frac{y^2}{2}\left[\frac{x n_z}{(1+n_z)^2}\right]+O(y^3) \ , \tag{5.17}$$

in which the first term is the reflected amplitude for a sharp surface (Fresnel's formula) and the remaining terms give the correction for the finite surface thickness a. We see that as $y \to 0$ the effect of the finite surface thickness is negligible and the DWBA reduces to Fresnel's formula. Thus this formula will be valid for essentially any surface as long as $q_z \ll 1/a$.

E. *Ad hoc* model of Pershan and Als-Nielsen

Neutron and x-ray reflectivity experiments are often analyzed on the basis of the *ad hoc* model

$$r=r_0 J'(q_z) \tag{5.18}$$

introduced by Pershan and Als-Nielsen.[17] We note that, since

$$r_0=\frac{x}{4}+O(x^2) \ , \tag{5.19}$$

this model, like the DWBA, reduces to the PWBA (5.14) as $x \to 0$, and since $J'(0)=1$ it also reduces to Fresnel's formula as $y \to 0$. Pershan later remarked[23] that "even though (the *ad hoc* model) cannot be formally justified . . . it is often applicable over all angles." In Sec. VI we determine the accuracy of both the DWBA and this *ad hoc* model by comparison with the exact reflectivity for a particular model surface.

VI. MODEL CALCULATIONS

For a given value of q_z, which depends on the experimental conditions, the reflectivity is uniquely determined by ρ and b, which are properties of the bulk material, and by the function $s(z)$ that characterizes the shape of the scattering length density in the neighborhood of the surface. In this section we consider a number of models of $s(z)$ for which the integrals in the PWBA and DWBA can be calculated analytically. We then use these models to illustrate how the reflectivity depends on the shape of $s(z)$, and to test the accuracy of the PWBA, the DWBA, and the *ad hoc* model of Pershan and Als-Nielsen.

A. Sharp surface

For a sharp surface,

$$s(z)=\delta(z) \tag{6.1}$$

and

$$\phi(z)=\begin{cases}1, & z>0\\ 0, & z<0 \ .\end{cases} \tag{6.2}$$

Hence $\xi_1=0$ and $J(q_z)=1$.

B. Step-function surface

For a step-function surface,

$$s(z)=\tfrac{1}{2}[\delta(z+a)+\delta(z-a)] \tag{6.3}$$

and

$$\phi(z)=\begin{cases}1, & z>a\\ \frac{1}{2}, & -a<z<a\\ 0, & z<-a \ .\end{cases} \tag{6.4}$$

Hence $\xi_1=1$ and

$$J(q_z)=\exp(iq_z a) \ , \tag{6.5}$$

so that

$$J'(q_z)=\cos(q_z a) \tag{6.6}$$

and

$$J''(q_z)=\sin(q_z a)\ . \tag{6.7}$$

C. Ramp-function surface

For a ramp-function surface,

$$s(z)=\begin{cases}0, & z>\sqrt{3}a\\ \dfrac{1}{2\sqrt{3}a}, & -\sqrt{3}a<z<\sqrt{3}a\\ 0, & z<-\sqrt{3}a\end{cases} \tag{6.8}$$

and

$$\phi(z)=\begin{cases}1, & z>\sqrt{3}a\\ \dfrac{1}{2}\left[1+\dfrac{z}{\sqrt{3}a}\right], & -\sqrt{3}a<z<\sqrt{3}a\\ 0, & z<-\sqrt{3}a\ .\end{cases} \tag{6.9}$$

Hence $\xi_1=\sqrt{3}/2$ and

$$J(q_z)=\frac{\exp(i\sqrt{3}q_z a)-1}{i\sqrt{3}q_z a}\ , \tag{6.10}$$

so that

$$J'(q_z)=\frac{\sin(\sqrt{3}q_z a)}{\sqrt{3}q_z a} \tag{6.11}$$

and

$$J''(q_z)=\frac{1-\cos(\sqrt{3}q_z a)}{\sqrt{3}q_z a}\ . \tag{6.12}$$

D. Error-function surface

For an error-function surface,

$$s(z)=\frac{1}{\sqrt{2\pi}a}\exp\left[-\frac{1}{2}\left[\frac{z}{a}\right]^2\right] \tag{6.13}$$

and

$$\phi(z)=\frac{1}{2}\left[1+\operatorname{erf}\left[\frac{z}{\sqrt{2}a}\right]\right], \tag{6.14}$$

where $\operatorname{erf}(x)$ is the error function[24]

$$\operatorname{erf}(x)=\frac{2}{\sqrt{\pi}}\int_0^x \exp(-t^2)dt\ . \tag{6.15}$$

Hence $\xi_1=\sqrt{2/\pi}$ and

$$J(q_z)=\exp[-\tfrac{1}{2}(q_z a)^2]\left\{1-\operatorname{erf}\left[-i\frac{q_z a}{\sqrt{2}}\right]\right\}, \tag{6.16}$$

so that

$$J'(q_z)=\exp[-\tfrac{1}{2}(q_z a)^2] \tag{6.17}$$

and

$$J''(q_z)=\frac{2}{\sqrt{\pi}}F\left[\frac{q_z a}{\sqrt{2}}\right], \tag{6.18}$$

in which $F(x)$ is Dawson's integral,[24]

$$F(x)=i\frac{\sqrt{\pi}}{2}\exp(-x^2)\operatorname{erf}(-ix)=\int_0^x \exp(t^2-x^2)dt\ . \tag{6.19}$$

E. Dependence of the reflectivity on the nature of $s(z)$

Figure 1 shows the normalized scattering length densities $\phi(z)$ for the models introduced above: the sharp surface (long-dashed line), the step-function surface (short-dashed line), the ramp-function surface (dotted line), and the error-function surface (solid line). In the latter three cases the surface thicknesses a are all the same ($q_c a=0.2$). The corresponding reflectivities are shown in Fig. 2. The results for the first two of these models are exact, given by Fresnel's (4.18) and Airy's formula,[5] while those for the latter two were obtained using the DWBA (5.12). This figure illustrates the variation of reflectivity with surface shape for a fixed surface thickness. Conversely, Fig. 3 shows the variation of reflectivity with surface thickness for a given shape. Here, the DWBA results for the error-function surface are shown by the dashed lines for $q_c a=0.1$, 0.2, 0.3, and 0.4. The exact result (4.18) for a sharp surface is shown by the solid line, and can be regarded as that for an error-function surface with $q_c a=0$.

Figures 2 and 3 demonstrate clearly the well-known fact that it is only when the momentum transfer q_z is well above the critical wave vector q_c that the reflectivity R is sensitive to the detailed shape and thickness of the sur-

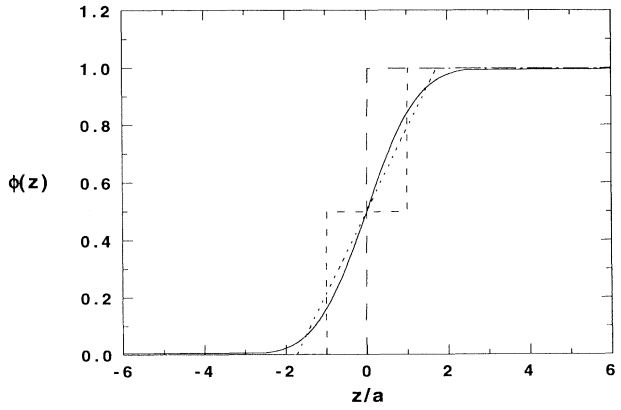

FIG. 1. Comparison of the normalized scattering length densities $\phi(z)$ for a sharp surface (long-dashed line), a step-function surface (short-dashed line), a ramp-function surface (dotted line), and an error-function surface (solid line). In the latter three cases $q_c a=0.2$.

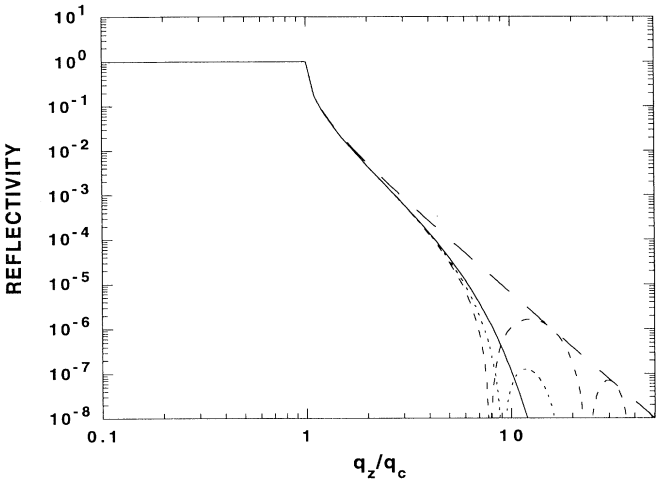

FIG. 2. Comparison of the reflectivities for a sharp surface (long-dashed line), a step-function surface (short-dashed line), a ramp-function surface (dotted line), and an error-function surface (solid line). In the latter three cases $q_c a = 0.2$. The first two cases are exact results, given by Fresnel's formula (4.18) and Airy's formula, and in the latter two the DWBA (5.12) was used.

face potential. In particular, one requires experiments with q_z/q_c ranging from about 3 to 30, where R decreases from about 10^{-3} to 10^{-7}, to obtain useful information on the shape and thickness of the surface potential. If $q_z \approx q_c$ the reflectivity depends only on the height of the potential barrier and is independent of the detailed shape of the potential near the surface.

F. Accuracy of the PWBA, DWBA, and *ad hoc* model

Since Airy's formula[5] provides an exact expression for the reflectivity of the step-function surface, it can be used

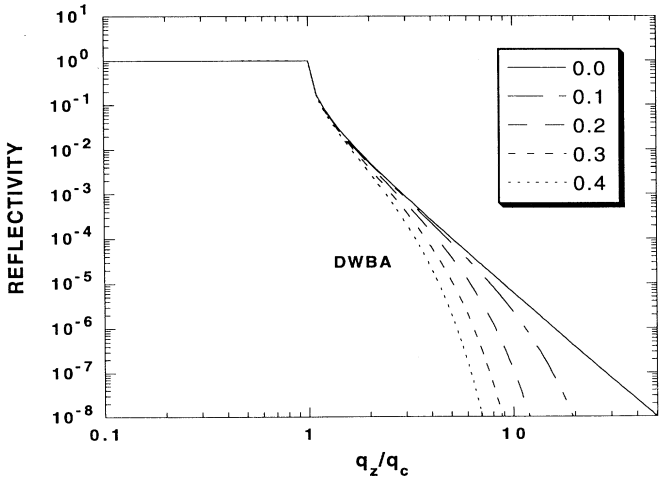

FIG. 3. Comparison of the DWBA (5.12) for an error-function surface with $q_c a = 0.1$, 0.2, 0.3, and 0.4 (dashed lines), with the exact result (4.18) for a sharp surface (solid line). The error-function surface reduces to a sharp surface in the limit $q_c a = 0$.

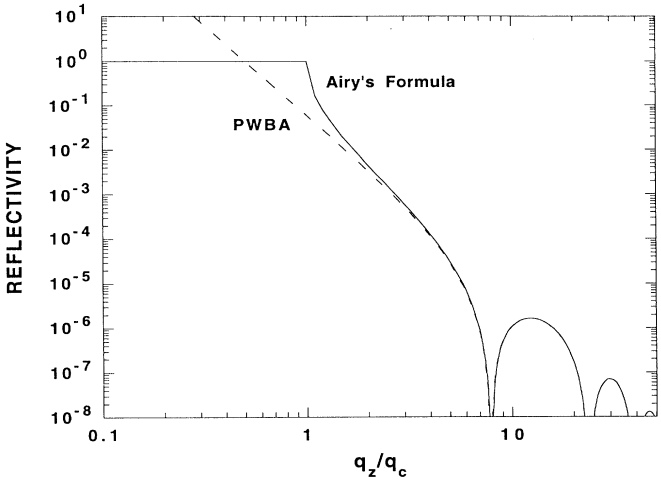

FIG. 4. Comparison of the exact reflectivity for a step-function surface with $q_c a = 0.2$, which is given by Airy's formula (solid line), with the PWBA (5.11) shown by the dashed line.

to test the accuracy of the PWBA (5.11), the DWBA (5.12), and the *ad hoc* model of Pershan and Als-Nielsen[17] (5.18).

Figure 4 compares the reflectivities calculated for a step-function surface with $q_c a = 0.2$ using Airy's formula (solid line) and the PWBA (dashed line). It is seen that in the region $q_z/q_c > 3$, where the reflectivity is sensitive to the detailed shape and thickness of the surface potential, the PWBA differs only slightly from the exact result. When the results for the DWBA are plotted as in Fig. 4, there is no noticeable deviation from the exact result at any value of q_z and, for the *ad hoc* model, there is only a barely perceptible deviation near q_c.

Figure 5 shows the absolute error, and Fig. 6 the relative error, as a function of q_z/q_c for the PWBA, the DWBA, and the *ad hoc* model. It is seen that in the region $q_z/q_c > 3$, where the reflectivity is sensitive to the

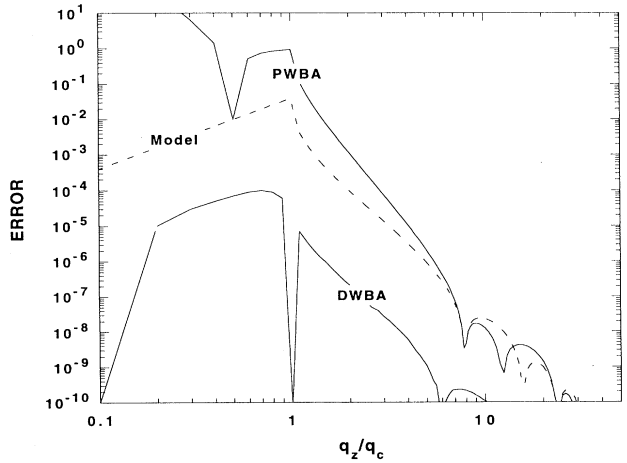

FIG. 5. Comparison of the absolute errors in the PWBA (5.11), the DWBA (5.12), and the *ad hoc* model (5.18) for a step-function surface with $q_c a = 0.2$.

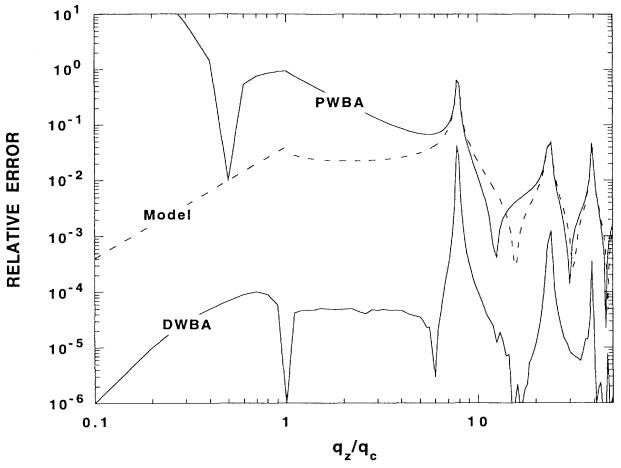

FIG. 6. Comparison of the relative errors in the PWBA (5.11), the DWBA (5.12), and the *ad hoc* model (5.18) for a step-function surface with $q_c a = 0.2$.

detailed shape and thickness of the surface potential, the *ad hoc* model is no better than the PWBA, the errors in both being typically of the order of 1%. The *ad hoc* model, however, is considerably more accurate than the PWBA at smaller values of q_z. The DWBA is typically three orders of magnitude more accurate than both the PWBA and the *ad hoc* model for all values of q_z, and the relative error in the DWBA is almost everywhere less than 0.01%. The only exceptions are near points where the exact reflectivity goes to zero and the relative error (Fig. 6) diverges. However, the absolute error (Fig. 5) is not anomalously large in these regions.

The expression (2.2) for the optical potential is itself not exact, but neglects local-field effects[18] which are also of the order of 0.01%. Thus the accuracy of the DWBA (5.12) is about the same as that of the Fermi pseudopotential, and both are adequate for essentially all practical purposes. Although we have only demonstrated this for the step-function surface, we feel it should be generally true for any symmetric surface.

VII. DISCUSSION

We have developed a theory for the specular reflection of thermal neutrons from an arbitrary smooth surface or interface using a Green-function technique that yields a formally exact expression (3.9) for the reflected amplitude. This leads to a family of Born approximations that includes both the familiar "plane-wave" Born approximation or PWBA, Eq. (4.7), and a generalized "distorted-wave" Born approximation or DWBA, Eq. (4.16).

The DWBA is a function of two dimensionless variables $x = (q_c/q_z)^2$ and $y = q_z a$, where q_z is the wave-vector transfer (which for specular reflection is normal to the surface, i.e., in the z direction), q_c is the critical wave vector for total reflection, and a provides a measure of the surface thickness. If $x \ll 1$ the DWBA reduces to the PWBA, and if $y \ll 1$ the DWBA reduces to Fresnel's formula for reflection from a sharp surface.

To demonstrate the dependence of the reflectivity on the shape and thickness of the surface potential, we have performed detailed numerical calculations of the reflectivity for a number of symmetric model surfaces: a sharp surface, a step-function surface, a ramp-function surface, and an error-function surface. These calculations show that it is only when $q_z \gg q_c$ that the reflectivity R is sensitive to the detailed shape and thickness of the surface potential. In particular, one requires experiments with q_z/q_c ranging from about 3 to 30, where R decreases from about 10^{-3} to 10^{-7}, to obtain useful information on the shape and thickness of the surface potential.

Since Airy's formula provides an exact expression for the reflectivity of the step-function surface, it can be used as a benchmark to test the accuracy of the PWBA (5.11), the DWBA (5.12), and the *ad hoc* model of Pershan and Als-Nielsen (5.18) for this surface. We find that the DWBA is typically three orders of magnitude more accurate than both the PWBA and the *ad hoc* model for all values of q_z, and that the relative error in the DWBA is almost everywhere less than 0.01%, which is, therefore, of the same order of magnitude as the intrinsic error in the Fermi pseudopotential itself.

The high accuracy that we have found when the DWBA is applied to symmetric scattering length densities, such as those in Fig. 1, is in contrast to the relatively low accuracy that Zhou, Chen, and Felcher[14,16] found when they applied this type of approximation to thin films on substrates. These authors emphasized[16] that the DWBA is valid only if the substrate has a high intrinsic reflectivity so that the Fresnel wave function (4.12) is a good first approximation to the actual wave function. This was not true for the models they examined, where the scattering length density in the films was much larger than in the substrates. However, it is true for the symmetric scattering length densities in Fig. 1. This evidently explains why, in our case, $f_1(z)$ is effectively a small perturbation and the DWBA works so well.

[1]G. P. Felcher, SPIE Conf. Proc. **983**, 2 (1988).
[2]J. Penfold and R. K. Thomas, J. Phys. Condens. Matter **2**, 1369 (1990).
[3]T. P. Russell, Mater. Sci. Rep. **5**, 171 (1990).
[4]M. Mâaza, C. Sella, and M. Kâabouchi, Appl. Surf. Sci. **60/61**, 573 (1992).
[5]M. Born and E. Wolf, *Principles of Optics*, 5th ed. (Pergamon, Oxford, 1975).
[6]L. Névot and P. Croce, Rev. Phys. Appl. **15**, 761 (1980).
[7]A. Steyerl, Z. Phys. **254**, 169 (1972).
[8]S. K. Sinha, E. B. Sirota, S. Garoff, and H. B. Stanley, Phys. Rev. B **38**, 2297 (1988).
[9]A. Steyerl, S. S. Malik, and L. R. Iyengar, Physica B **173**, 47 (1991).
[10]W. A. Hamilton and R. Pynn, Physica B **173**, 71 (1991).
[11]R. Pynn, Phys. Rev. B **45**, 602 (1992).

[12]P. Mazur and D. L. Mills, Phys. Rev. B **26**, 5175 (1982).
[13]S. Dietrich and H. Wagner, Z. Phys. B **59**, 35 (1985).
[14]X. L. Zhou, S. H. Chen, and G. P. Felcher, J. Phys. Chem. **95**, 9025 (1991).
[15]X. L. Zhou, G. P. Felcher, and S. H. Chen, Physica B **173**, 167 (1991).
[16]X. L. Zhou, S. H. Chen, and G. P. Felcher, Phys. Rev. A **46**, 1839 (1992).
[17]P. S. Pershan and J. Als-Nielsen, Phys. Rev. Lett. **52**, 759 (1984).
[18]V. F. Sears, *Neutron Optics* (Oxford University Press, New York, 1989).
[19]B. A. Lippmann and J. Schwinger, Phys. Rev. **79**, 469 (1950).
[20]For the case of a thin film on a substrate, Eq. (3.9) reduces to the result obtained in Ref. 15.
[21]V. F. Sears, Acta Crystallogr. A **39**, 601 (1983).
[22]S. W. Lovesey, *Theory of Neutron Scattering from Condensed Matter* (Clarendon, Oxford, 1984).
[23]P. S. Pershan, J. Phys. (Paris) Colloq. **50**, C7-1 (1989).
[24]M. Abramowitz and I. A. Stegun, *Handbook of Mathematical Functions* (National Bureau of Standards, Washington, D.C., 1965).